
Lymphocytes Studied by Raman Microspectroscopy

Magdalena Pietruszewska, Grażyna Biesiada,
Jacek Czepiel, Malwina Birczyńska, Paulina Moskal,
Mateusz Kozicki, Emilia Hola,
Aleksander Garlicki and
Aleksandra Weselucha-Birczyńska

Additional information is available at the end of the chapter

<http://dx.doi.org/10.5772/intechopen.81895>

Abstract

The Raman spectroscopy detects the interaction of the incident light with the electrons in the illuminated molecule. The use of Raman spectroscopy to investigate biological molecular structures and the recognition of their particular functional groups have been growing rapidly, and nowadays the use of Raman spectroscopy has expanded toward the cellular level. The activation of lymphocytes occurs when they are exposed to viruses or other foreign antigens. We have observed that Raman spectroscopy can be used to screen the activation of lymphocytes during viral infection. We have indicated the bands that reveal differences between activated and intact cells. The most important marker of the lymphocyte activation process is the prominent 521 cm^{-1} disulfide band which marks the immunoglobulin formation. The blood from the patients with viral infections, e.g., mononucleosis, and from healthy volunteers was obtained by venipuncture during hospitalization in the University Hospital in Kraków.

Keywords: Raman microspectroscopy, viral infection, activation of lymphocytes

1. Introduction

The proper functioning of the immune system results from close cooperation of the mechanisms of nonspecific (innate) immunity and adaptive immunity (acquired) [1]. Both mechanisms operate by direct contact between the cells and through interactions in which cytokines or chemical mediators participate.

The basic task of the immune system is to detect the hazard in the form of foreign antigens, infectious agents, or their own altered cells that have been infected or transformed, for example, by cancer. To distinguish between self and foreign antigens, the host organism engages specific and nonspecific response cells showing the presence of appropriate receptors. Nonspecific response receptors recognize a very wide range of structure characteristics for infectious agents that are not produced in higher organisms. These are pathogen-associated molecular patterns (PAMP) or microbe-associated molecular patterns (MAMP). The specific response receptors behave differently. They recognize highly specific antigen fragments, single epitopes. They are B cell receptors (BCR) and antibodies and also T cell receptors (TCR) of T lymphocytes.

Lymphocytes are totally responsible for specific immunological recognition of pathogens [2]. They initiate a specific immune response. All cells derived from myeloid stem cells but T lymphocytes then develop in the thymus, while B cells develop in the bone marrow. Each B cell is programmed to express on the surface of receptors specific for a particular antigen. Antibodies neutralize foreign factors due to specific binding to antigens [3].

Advances in microspectroscopic techniques have contributed to a new insight of the molecular environment for lymphocyte activation [4]. The explanation of the immunological synapse function, which influences the B cell acquisition of membrane-attached antigens, was explained with the use of three-dimensional confocal microscopy (3D-CM) [5]. Infrared microspectroscopy and Raman microspectroscopy are new methods that give the opportunity to observe human cells, tissues at the molecular level, and give the opportunity to examine physiological and pathological changes [6–17]. Revealing even small spectral differences between distinct regions of a cell, vibrational spectroscopy provides considerable potential as a rapid screening method [8, 18].

Raman spectroscopy, with an important contribution of resonance Raman phenomenon by using certain chromophores, can be applied to resolve certain chemical species and can be considered as a diagnostic method [6, 19].

Raman spectroscopy is able to give some insight into the functioning of the immune system. Some worth mentioning guidelines in B and T cell lymphocytes differentiation is described in the Hobro et al. work [20], although the authors conclude that the misclassification rate is relatively high. Being aware that the immune response may be very complex, it is of interest to establish how a virus infection and single lymphocyte cell activation by Raman spectroscopy are visible.

2. Blood samples

We have studied two types of viral diseases, influenza and infectious mononucleosis.

The healthy volunteers constitute the reference group. The infectious patients were treated in the Department of Infectious Diseases, Jagiellonian University Hospital in Kraków.

The blood was deposited as a film to measure. The cells were allowed to settle for about 10 minutes prior to measurement.

The studies were conducted in accordance with the guidelines for good clinical practice (GCP) according to the ethical principles for medical research involving human subjects (Declaration of Helsinki). The study was approved by the local bioethical committee.

3. Single cell measurements by Raman spectroscopy

Raman spectra were collected using a Renishaw inVia spectrometer, working in confocal mode, connected to a Leica microscope. A 785-nm HP NIR (high-power near IR) diode laser and a 514.5-nm Ar⁺ laser were used to excite the samples. The laser beam was focused by a 100-fold magnifying glass, the high-class Leica objective for standard applications, with a large numerical aperture (NA = 0.9). The laser power was kept low, ca. 1–3 mW at the sample, to ensure a minimum invasion of cells.

During the point mapping experiments, the sample was shifted on a motorized stage (Prior Scientific) at fixed intervals within the defined area. For the mapping experiments, the factory-supplied software was used (Renishaw, WiRE v. 2.0 and 3.4). The Raman images are based on Raman intensities.

Principal component analysis (PCA) was applied to determine the variance between the Raman spectra of a single lymphocyte of a patient with identified early stage of infectious mononucleosis and healthy donors. PCA was performed in the whole spectral region with the Unscrambler X software packages (v. 10.3, CAMO Software, Oslo, Norway). The Raman spectra were smoothed using a Savitzky-Golay smoothing algorithm (13 smoothing points), baseline corrected and unit vector normalized.

The first principal component, PC-1, contains the highest percentage of variation, which indicates the direction of the maximum variation in the dataset.

4. Raman spectra of naive lymphocytes

Lymphocytes carry out immune surveillance, that is, they constantly monitor tissues for the presence of foreign antigens [21]. The human body continuously produces new cells. They circulate between blood and lymph, not only by lymphatic organs but also to a lesser extent by other body tissues [22]. It takes around 24 hours to complete the circulation. Circulating lymphocytes are a group composed of small, long-living cells. The continuous movement of these lymphoid cells means that they are always available for immune defense [3].

The circulatory route of naive lymphocytes T and B is different from that of the memory and effector lymphocytes. In the pool of circulating lymphocytes, the majority of cells are immune memory T cells [21]. The B lymphocytes account for only 15% of the total pool of circulating lymphocytes. Their circulatory pathways are still not well understood.

Cellular processes may be monitored using Raman spectroscopy exploiting the chemical specificity of using the high polarizability of certain functional groups that build molecular cell systems [22–24]. No staining is necessary to observe the diversity of areas inside the cell [25]. The

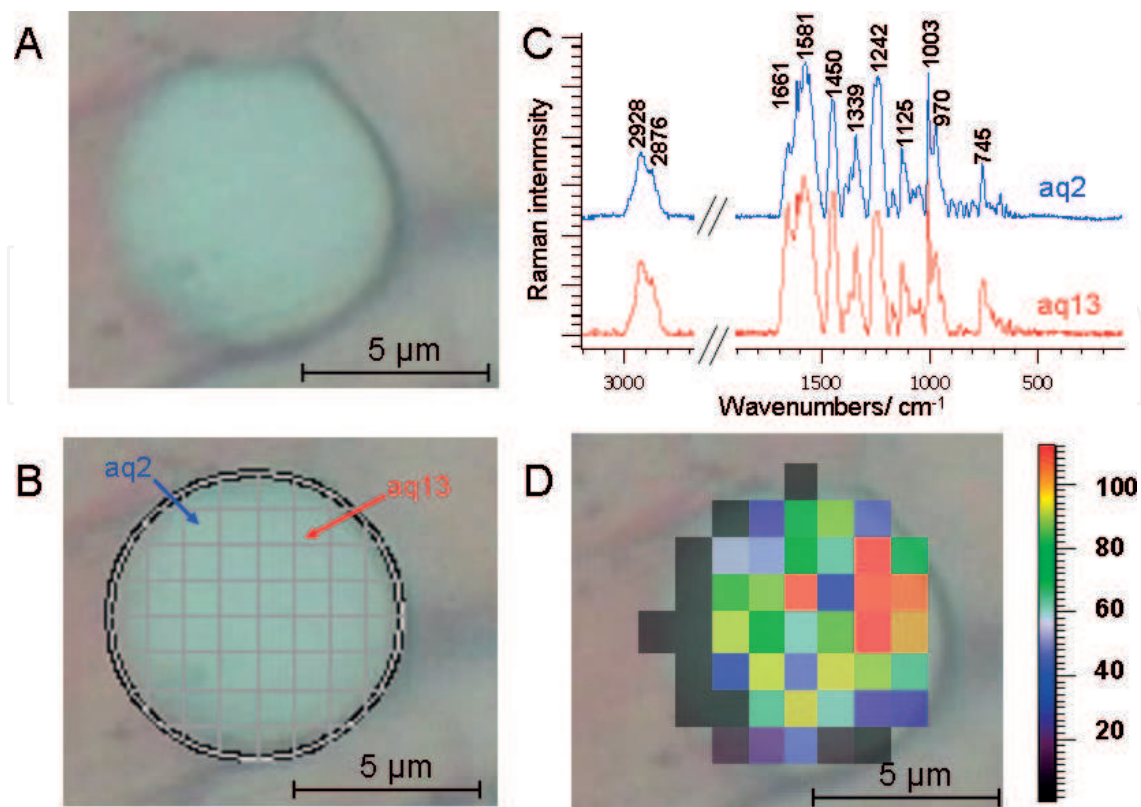


Figure 1. The single, naive human lymphocyte. (A) A photomicrograph (reflected light, objective 100×); (B) with the marked region over which the map experiment was performed; (C) Raman spectra of the sample area including the cell membrane (aq3) and the center of the cell (aq13); and (D) distribution of proteins in the lymphocyte (1660 cm⁻¹ marker band), excitation laser line 785 nm.

Raman bands [cm ⁻¹]				Assignment [7–18, 25, 33, 34, 38, 41]
785 nm	785 nm	785 nm	514.5 nm	
Naïve	Activated (influenza)	Activated (EBV)	Activated (EBV)	
2926	2926	2933	2937 (aq13) 2932 (aq6)	CH sym str of CH ₃ methyl group
2875	2875	2889	2878 (aq13) 2874 (aq6)	CH asym. str of CH ₂ methylene group
1662 (aq2) ↓ 1662 (aq13) ↑	1657 (aq41) ↑ 1657 (aq3) ↓	1661	1657 (aq13) 1664 (aq6)	Amide I
1617			1617	Tyr
1581	1581	1578	1581	G, A, nucleic acids, Trp, Phe
1450	1450 (aq41) ↑	1450	1452 (aq6)	CH ₂ deformation modes, proteins and lipids
1339	1340	1342		A, CH deformations, nucleic acids and proteins
1243	1246	1254	1241	A, Amide III
1123	1125	1132		CN str
—	1100	1100		PO ₂ ⁻ phosphate backbone vibration (DNA marker)

Raman bands [cm ⁻¹]				Assignment [7–18, 25, 33, 34, 38, 41]
785 nm	785 nm	785 nm	514.5 nm	
Naïve	Activated (influenza)	Activated (EBV)	Activated (EBV)	
1031	1031	1035		Phe, C—H in-plane stretching
1003	1003	1005	1005	Phe, ring breathing mode
970	970			CC, skeletal mode
855/835	855 (aq41) ↑	855		Tyr, buried/ exposed
751 (aq2)	740 (aq41)	754 (aq5)↑		T-ring breathing, nucleic acids, Trp
747 (aq13)	752 (aq3)			
620 (aq13)	620 (aq3)	621 (aq5)↑		C—S stretching mode, Phe, His
	617 (aq41)	610 (aq8)		
587 (aq13)				S—S disulfide bridge, Trp
521	521 (aq41) ↑	521	520 (aq13)	V _L domain S—S bridge

A, adenine; G, guanine; T, thymine; Phe, phenylalanine; Tyr, tyrosine, Trp, tryptophane; His, histidine.

Table 1. Assignments of significant Raman bands observed for human lymphocyte (785 and 514.5 nm excitation laser line).

membrane of the cell (e.g., aq2) clearly differs from the center (e.g., aq13) (**Figure 1C and D**); this variation is related to the lower presence of protein in the cell membrane, estimated by the intensity of the amide I band. The middle area is relatively homogeneous due to the distribution of proteins, which indicates fully mature cell (**Figure 1D**). The significant Raman bands observed for human lymphocytes and their assignments are collected in **Table 1**.

5. Immunity against viruses

Viruses are usually small compared to other organisms that cause infection; their metabolism is closely dependent on the host’s metabolism [26]. That is why viruses are not capable of replicating themselves. Therefore, the key process in viral infection is intracellular replication, which can even lead to the death of infected cells.

Antibodies prevent the penetration of the virus into an uninfected cell and thus limit some viral infections that spread with the blood.

6. Influenza and its etiology

Influenza is an acute illness of the respiratory system caused by influenza viruses that belong to the *Orthomyxoviridae* family. They are divided into three types A, B, and C on the basis of antigenic features of nucleoprotein and matrix protein antigens [27].

The host’s response to flu infection is a complex system of dependencies between humoral immunity, local antibody production, cellular immunity, and other mechanisms. The presence

of antibodies confirming the response to the infection is established in biochemical tests, the most important of which is hemagglutination inhibition (HI) test.

7. Infectious mononucleosis and its etiology

EBV virus induces an infectious mononucleosis characterized by heterophilic antibodies, fever, sore throat lymphadenopathy, and atypical lymphocytosis [28]. The virus belongs to the family *Herpesviridae*. The viral genome is a double-stranded DNA with a linear system, surrounded by a nucleocapsid with an icosahedral symmetry; on the outside there is a capsule containing glycoprotein.

More than 90% of adults report the presence of antibodies to EBV infection. An EBV is transmitted with saliva. The infection of B lymphocytes present in the tonsils crypts may take place directly; the next stage is blood virus spreading. There is observed lymphoid tissue growth due to EBV infected B lymphocytes proliferation and the accompanying T-cell reaction.

8. Raman spectrum of activated lymphocytes in response to the influenza virus

Once naive lymphocytes have been exposed, they are activated. This is an important element in the humoral immune response of the body. Free antibodies present in the blood, in the lymph, in all body fluids, and in secretions are involved in this process [1].

They are produced by B cells, initially functioning as APC, which, due to cooperation with Th2 lymphocytes, are transformed into clones of plasma cells producing antigen-specific antibodies [29]. Although antibodies do not destroy infectious agents but they bind epitopes in a specific way, so they are able to initiate effector mechanisms and eliminate the pathogen from the host organism.

That is why LeBien and Tedder commented that the discovery of B cells did not result from cell identification, but rather the identification of a protein, that is, immunoglobulin or antibody [30].

As a response to increased lymphocyte activation, a significant change in their shape and behavior is detected (compare **Figure 1A** and **Figure 2A**). Some of the stimulated B lymphocytes become active in the production of antibodies against foreign antigens, and they are transformed into plasma cells (compare **Figure 1D** and **Figure 2D**). This process allows the immune system to recognize infectious agents and prepare responses to them.

The spectroscopic marker of the lymphocyte activation process is a prominent 521 cm^{-1} disulfide band which marks the formation of the immunoglobulin (**Figure 2C**, aq41).

Immunoglobulin, initially present in the cytoplasm and then bound to the surface, is the main feature of B lymphocytes. They are used to identify specific antigens [26]. Immunoglobulins,

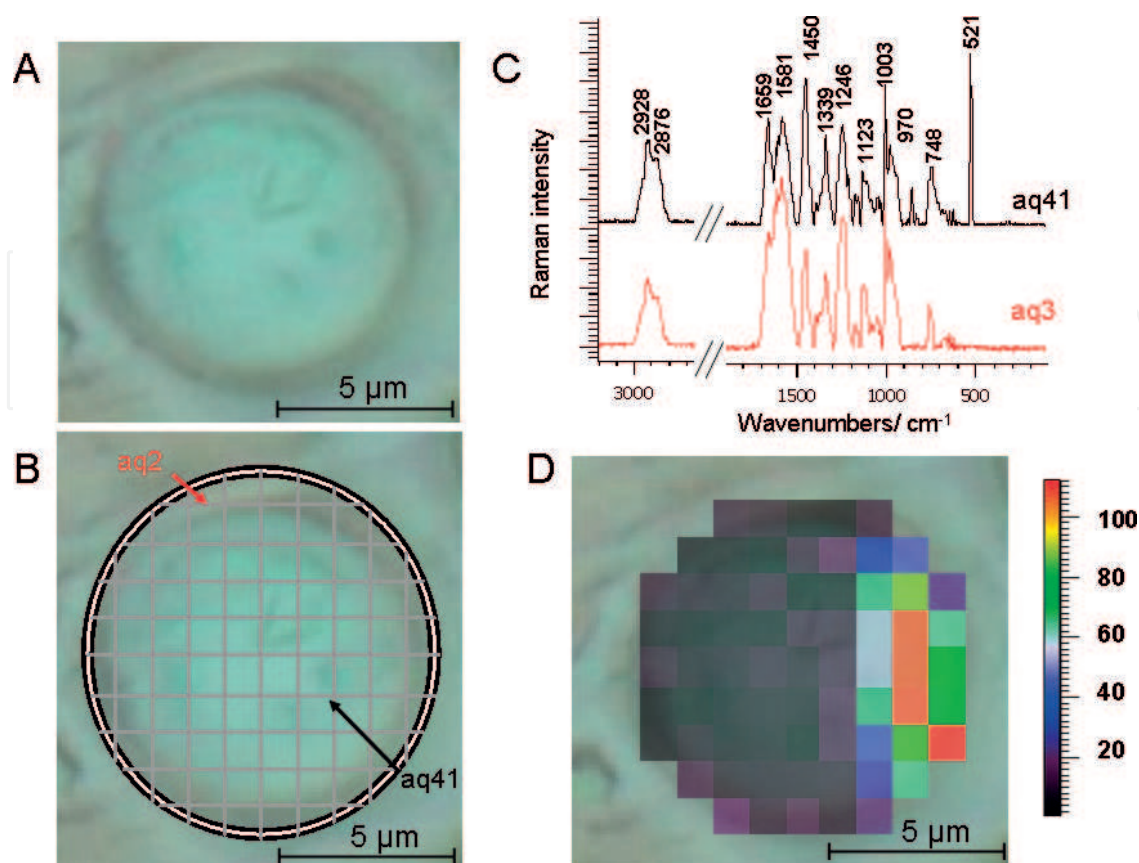


Figure 2. Activated B lymphocyte in response to the influenza virus. (A) A photomicrograph (reflected light, objective 100×); (B) with the marked region over which the map experiment was performed; (C) Raman spectra from an exemplary area including nonactivated (aq2) and from the activated region of the cell (aq41); and (D) distribution of immunoglobulins in the lymphocyte (map created from 521 cm⁻¹ marker band), excitation laser line 785 nm.

regardless of function, have a similar molecular structure as well as basically identical mechanism of reacting with antigen [21]. They are all built from the same basic units, light (L) and heavy (H) polypeptide chains [31]. The basic immunoglobulin unit is a tetramer consisting of two identical heavy chains and two light chains. The two heavy chains are linked to each other by disulfide bonds, in so-called hinge region, and each heavy chain is linked to a light chain by a disulfide bond (**Figure 3**). The disulfide bond is a structural feature of many significant biological molecules, because it provides additional stability to a protein molecule. Therefore, the structural characteristics of the CS—SC dihedral angle and the structure of the entire molecule are important [32].

Raman spectroscopy is the best spectroscopic technique to monitor the disulfide bonds and the structure and conformation of a protein [33, 34]. Compounds containing disulfide bonds usually show well-defined bands in the Raman spectra that arise from C—S and S—S stretching modes that are also sensitive to the CS—SC dihedral angle [32]. Additionally, they appear in a region of the Raman spectrum that is relatively free from other intense bands. The experimental Raman data can be correlated with X-ray data and the results obtained from calculations [35–38].

The spatial structure within the N-terminal section of the H and L chains makes it extremely important [21]. It is now known that one antibody molecule may bind to two or more

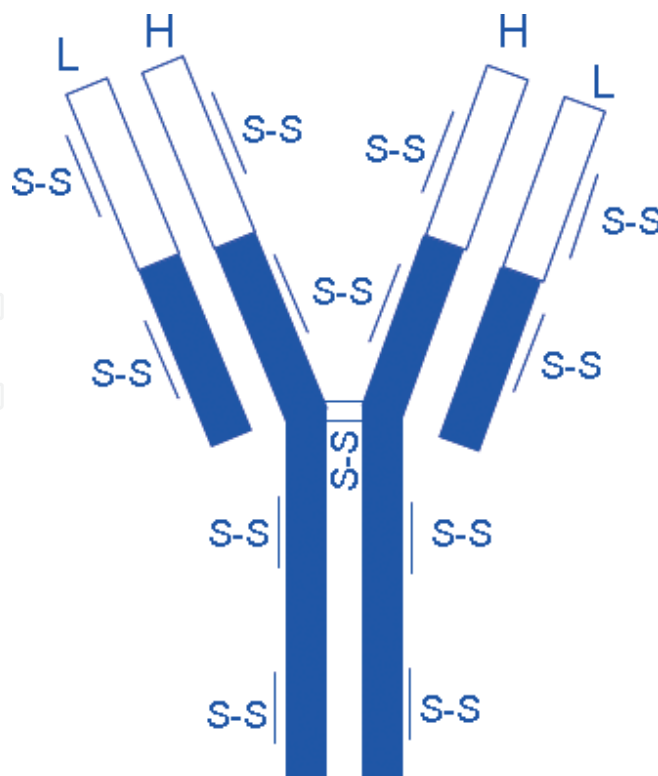


Figure 3. Diagram of the molecular structure of the immunoglobulin molecule.

completely different chemical determinants, which indicates that the anti-determinant does not directly recognize the specific chemical configuration of the antigen, but its overall spatial shape. Therefore, the role of Raman spectroscopy, which makes it possible to determine the structure, seems to be very promising.

Activation of lymphocytes, marked by the appearance of an immunoglobulin, also manifests itself as changes in the cell content. The peak of ca. 1130 cm^{-1} (protein C—N str.) loses its intensity as well as 1100 cm^{-1} phosphate backbone vibration, indicating DNA concentration [9]. These spectral changes signify the lymphocyte evolution toward the plasma cell, which has a small eccentric nucleus, and most of the cell is filled by cytoplasm and well-developed rough endoplasmic reticulum (RER) where immunoglobulin synthesis takes place.

This is in agreement with the presence of intense lipid Raman bands at 1450 cm^{-1} in plasmocytes (because of RER).

Another important Raman band, amide I (C=O stretching and N—H bending vibrations) at 1662 cm^{-1} , is more intensive (**Table 1**). This position indicates that immunoglobulin in the intact form is predominantly composed of antiparallel β -sheet structure [33]. The protein composition seems to be different in activated form as amide I band intensity is slightly shifted toward lower wave numbers (**Table 1**).

A further characteristic band, which occurs as well in naive lymphocytes as in the activated form, is the 850 cm^{-1} peak due to the exposed tyrosine residues in the proteins (**Table 1**) [33]. Tyrosine is an important amino acid in signal transduction and regulating cellular activity (by tyrosine kinase) [39].

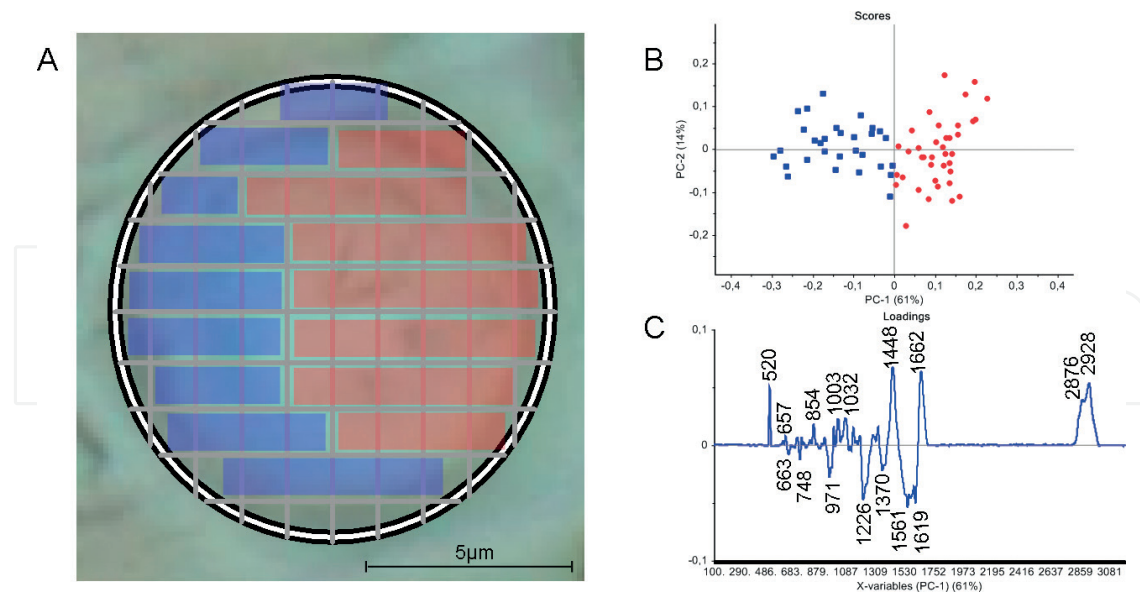


Figure 4. The results of PCA applied to Raman spectra of activated (red dots) and nonactivated (blue dots) B lymphocyte regions in the spectral range 3200–100 cm^{-1} showing (A) a photomicrograph (reflected light, objective 100 \times) with marked activated (red) and non-activated (blue) regions; (B) scores plot for PC-1 and PC-2 (C) loadings plot for PC-1, excitation laser line 785 nm.

The principal component analysis (PCA) was applied to distinguish two areas of the B cell, classified as activated, and the one in which the presence of an immunoglobulin is not yet manifested (**Figure 4**). The PCA used to reduce the large amount of spectral information contained in the Raman spectra into a few principal component parameters. The activated area is characterized by PC-1 up to 61%.

Lymphocyte activation is defined by Raman bands:

- 520 cm^{-1} (disulfide band)
- 657 cm^{-1} (Tyr)
- 854 cm^{-1} (Tyr, exposed)
- 1003 cm^{-1} and 1032 cm^{-1} (Phe)
- 1448 cm^{-1} (CH_2 def., lipids)
- 1662 cm^{-1} (amide I, β -sheet conf.)
- 2876 cm^{-1} (CH asym str, in CH_2)
- 2928 cm^{-1} (CH sym str, in CH_3)

The following bands are specified for the nonactivated lymphocyte area:

- 663 cm^{-1} (CS str)
- 748 (T, nucleic acids)

- 971 cm^{-1} (CC, structurally sensitive mode)
- 1226 cm^{-1} (CH_2 def.)
- 1370 cm^{-1} (T, A, G, nucleic acids, Trp, Phe, CH_2 , and CH_3 def.)
- 1561 cm^{-1} (amide II, His)
- 1619 cm^{-1} (Tyr)

9. Raman spectrum of activated lymphocytes in response to the EBV virus infection

The B cell activated in EBV infection and distribution of immunoglobulin is presented in **Figure 5** (785 nm laser line) and **Figure 6** (514.5 nm laser line). The marker for cell activation is the 521 cm^{-1} immunoglobulin band. The plasma cell shown in **Figure 5** reveals relatively uniformly activated cell. The position of the immunoglobulin marker indicates that this band characterizes the disulfide bridge in the domain of the V_L light chain (**Table 1**). Similar results were received for immunoglobulin in activated lymphocytes in influenza.

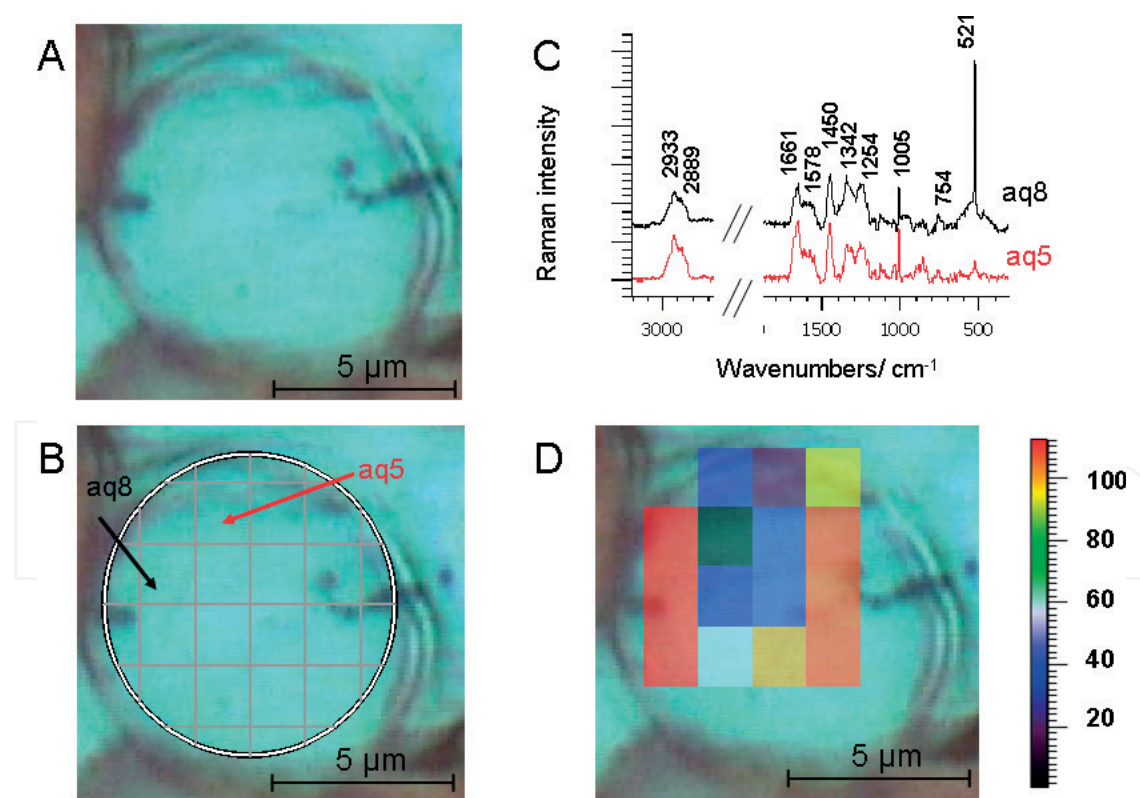


Figure 5. Activated B lymphocyte in response to the EBV virus. (A) A photomicrograph (reflected light, objective 100 \times); (B) with the marked region over which the map experiment was performed; (C) Raman spectra from an exemplary area including the nonactivated (aq5) and from the activated regions of the cell (aq8); and (D) distribution of immunoglobulins in the lymphocyte (map created from 521 cm^{-1} marker band), excitation laser line 785 nm.

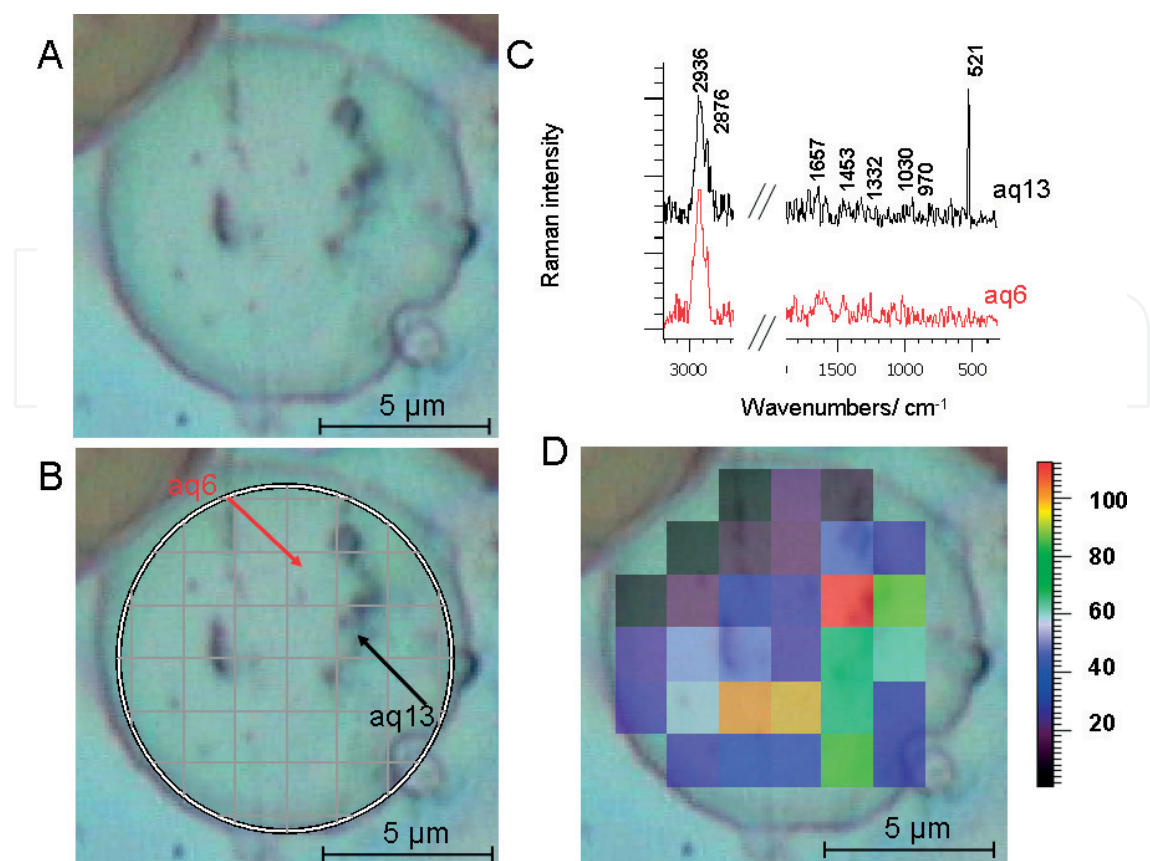


Figure 6. Activated B lymphocyte in response to the EBV virus. (A) A photomicrograph (reflected light, objective 100×); (B) with the marked region over which the map experiment was performed; (C) Raman spectra from an exemplary area including the nonactivated (aq6) and from the activated regions of the cell (aq13); and (D) distribution of immunoglobulins in the lymphocyte (map created from 521 cm^{-1} marker band), excitation laser line 514.5 nm.

The PCA model was built based on spectra recorded for lymphocyte B for the two research groups, at the beginning of hospitalization due to EBV infection and after receiving medical tests indicative of recovery (**Figure 7A**) [40]. The PCA score plots show a separation based on differences in the lymphocytes' content for these two research groups.

Maxima bands in the loadings plot (**Figure 7B**) at wave number values of 3175 and 2891 cm^{-1} are assigned to vibrations of the CH and antisymmetric C—H stretching vibrations of methyl and methylene groups which originate from lipids in the EBV-activated cells. The shifts observed in the protein modes at 1638 and 1673 cm^{-1} in the loading plot for EBV activated and not activated B cells, respectively, are possibly indicative of a difference in protein secondary structure between the two experimental groups. The positive loading at 750 cm^{-1} correlated with positive scores along PC-4 indicates predominance of nucleic acids in activated lymphocytes. It must be noted that the fourth principal component, PC-4 that separates classified groups, counts only 1% variation for spectral dataset analyzed in the whole range. When a narrower range is analyzed, an important component becomes PC-1 that sums 37% of variation (**Figure 7C**). Perhaps, this indicates the specificity of EBV pathogenesis and the formation of latent form in the B cell.

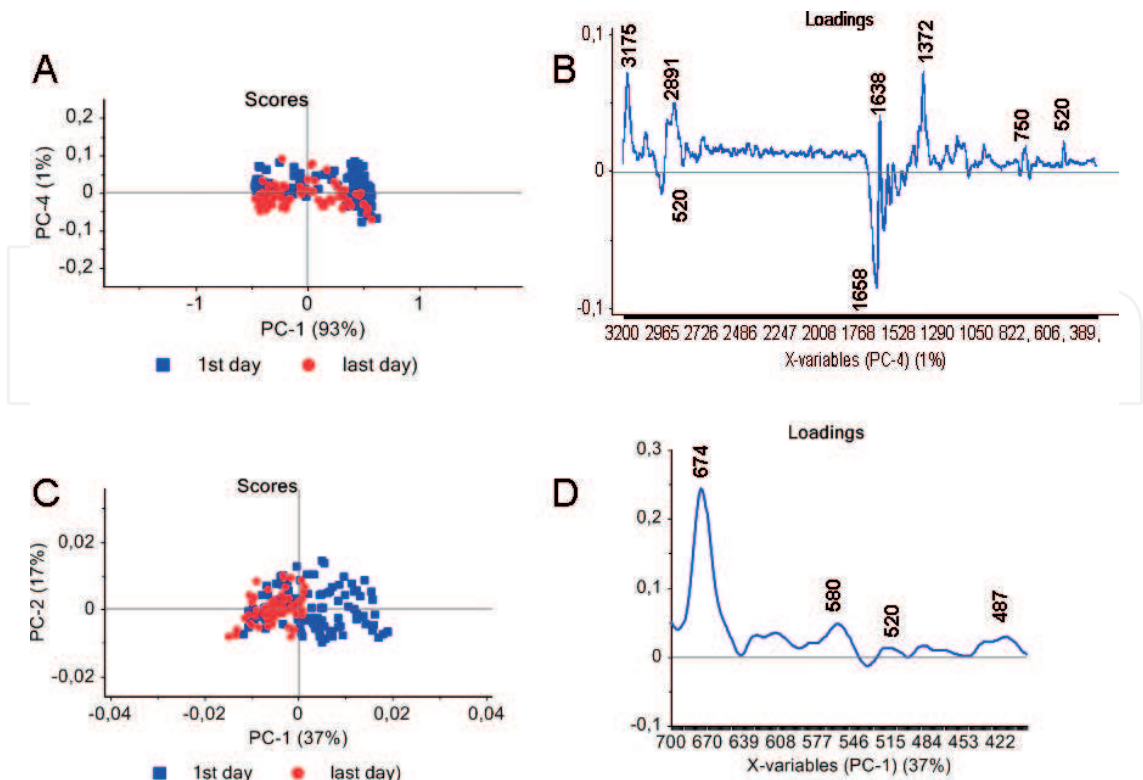


Figure 7. The results of PCA applied to Raman spectra at the beginning of hospitalization due to infectious mononucleosis (blue dots) and after the symptoms of infection have stopped (red dots), (A) in the spectral range 3200–300 cm^{-1} showing scores plot PC-1 vs. PC-4 and (B) loadings plot for PC-4 and (C) in the spectral range 700–400 cm^{-1} showing scores plot PC-1 vs. PC-2 and (D) loadings plot for PC-1, excitation laser line 514.5 nm.

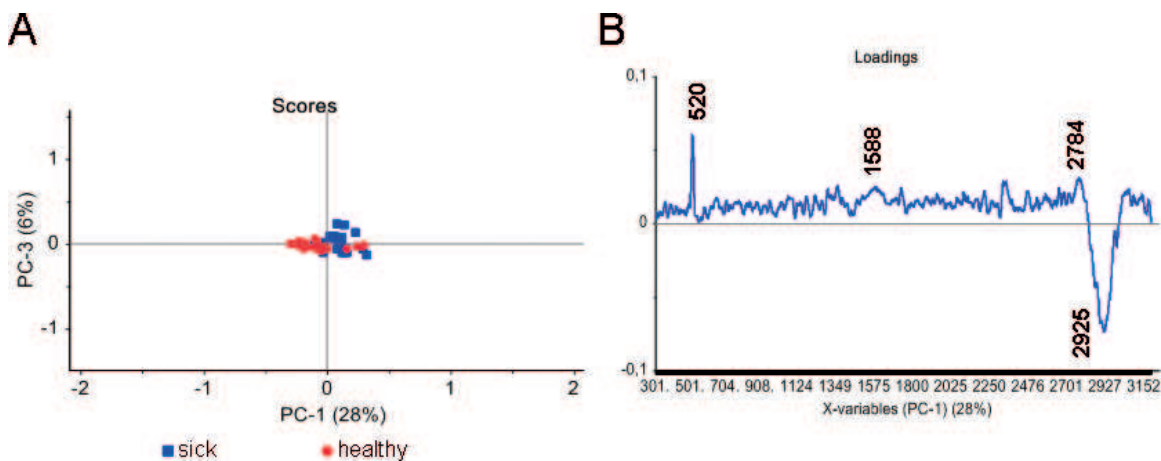


Figure 8. The results of PCA applied to Raman spectra of naïve (red dots) and activated B lymphocytes in response to the EBV virus (blue dots) in the spectral range 3200–300 cm^{-1} showing (A) scores plot for PC-1 and PC-3 and (B) loadings plot for PC-1, excitation laser line 514.5 nm. The magnetic labeling was used to separate B cells from the whole blood (Miltenyi Biotec, Germany).

Figure 8 presents the results of PCA model of Raman spectra of naïve and activated B lymphocytes in response to the EBV virus in the spectral range 3200–300 cm^{-1} . The examined cells were separated from the whole blood using the magnetic B lymphocyte labeling system.

10. Conclusions

In the case of flu infection, the presence of antibodies in the serum can be confirmed by hemagglutination inhibition (HI) test, in complement fixation (CF) or neutralization reaction, and also using ELISA, the enzyme immunoassay [1]. Using these biochemical methods, antibodies are recorded only after 1 week. Raman spectroscopy gives this information, at the level of a single cell, immediately when single cell is activated.

Raman spectroscopy allows to identify a B lymphocyte. Once stimulated by binding to a foreign antigen, for example, virus, a lymphocyte is getting ready to multiply into a clone of identical cells.

On the other hand, it allows immediately to determine that B lymphocyte was in contact with the virus by the appearance of the 521 cm^{-1} marker band.

Antibody molecule may not directly recognize the specific chemical configuration of the antigen, but its overall spatial shape; therefore, the role of Raman spectroscopy, which makes possible to determine the structure, seems to be very promising.

The character of considered viral infections is different. In Raman spectra, we can observe it in PCA. The fact that only less than 40% for EBV is separated, between ill and control recovery groups, could be due to a latent form of EBV virus. In influenza the observations were different—there were about 60% PC factor-separating data.

Acknowledgements

MP acknowledges the support of InterDokMed project no. POWR.03.02.00-00-I013/16.

MB acknowledges the support of the same InterDokMed project no. POWR.03.02.00-00-I013/16.

Author details

Magdalena Pietruszewska¹, Grażyna Biesiada^{2,3}, Jacek Czepiel^{2,3}, Malwina Birczyńska^{2,3}, Paulina Moskal¹, Mateusz Kozicki¹, Emilia Hola¹, Aleksander Garlicki^{2,3} and Aleksandra Weselucha-Birczyńska^{1*}

*Address all correspondence to: birczyns@chemia.uj.edu.pl

1 Faculty of Chemistry, Jagiellonian University, Kraków, Poland

2 Department of Infectious and Tropical Diseases, Jagiellonian University, Medical College, Kraków, Poland

3 Department of Infectious Diseases, The University Hospital in Kraków, Kraków, Poland

References

- [1] Gieryńska M. Resistance mechanisms in viral infections. In: Wróblewska M, Dziwiątkowski T, editors. *Viral Diseases in Clinical Practice* (in Polish). Warszawa: PZWL; 2017
- [2] Male D, Brostoff J, Roth DB, Roitt I. *Immunology*, Seventh ed. Elsevier; 2006
- [3] Stevens A, Lowe JS. In: Zabel M, editor. *Human Histology*. 2nd ed. Warszawa, Poland: Wydawnictwo Lekarskie PZWL & Wydawnictwo Medyczne Słotwiński Verlag; 2000
- [4] Roda-Navarro P. Microspectroscopy reveals mechanisms of lymphocyte activation. *Integrative Biology*. 2013;**5**:300-311
- [5] Batista FD, Iber D, Neuberger MS. B cells acquire antigen from target cells after synapse formation. *Nature*. 2001;**411**:489-494
- [6] Ellis DI, Goodacre R. Metabolic fingerprinting in disease diagnosis: Biomedical applications of infrared and Raman spectroscopy. *Analyst*. 2006;**131**:875-885
- [7] Chan JW, Taylor DS, Zwerdling T, Lane SM, Ihara K, Huser T. Micro-Raman spectroscopy detects individual neoplastic and normal hematopoietic cells. *Biophysical Journal*. 2006;**90**:648-656
- [8] Krafft C, Knetschke T, Siegner A, Funk RHW, Salzer R. Mapping of single cells by near infrared Raman microspectroscopy. *Vibrational Spectroscopy*. 2003;**32**:75-83
- [9] Notingher I. Raman spectroscopy cell-based biosensors. *Sensors*. 2007;**7**:1343-1358
- [10] Czepiel J, Kozicki M, Panasiuk P, Birczyńska M, Garlicki A, Weselucha-Birczyńska A. *Clostridium difficile* the hospital plague. *Analyst*. 2015;**140**:2513-2522
- [11] Kozicki M, Creek DJ, Sexton A, Morahan BJ, Weselucha-Birczyńska A, Wood BR. An attenuated total reflection (ATR) and Raman spectroscopic investigation into the effects of chloroquine on *Plasmodium falciparum*-infected red blood cells. *Analyst*. 2015;**140**(7):2236-2246
- [12] Kozicki M, Czepiel J, Biesiada G, Nowak P, Garlicki A, Weselucha-Birczyńska A. The ring-stage of *Plasmodium falciparum* observed in RBCs malaria hospitalized patients. *Analyst*. 2015;**140**:8007-8016
- [13] Weselucha-Birczyńska A, Sacharz J, Zięba-Palus J, Lewandowski MH, Kowalski R, Palus K, et al. The application of Raman microspectroscopy for the study of healthy rat brain tissue. *Vibrational Spectroscopy*. 2016;**85**:48-54
- [14] Zięba-Palus J, Weselucha-Birczyńska A, Sacharz J, Lewandowski MH, Palus K, Chrobok Ł, et al. 2D correlation Raman microspectroscopy of chosen parts of rat's brain tissue. *Journal of Molecular Structure*. 2017;**1147**:310-316
- [15] Sacharz J, Weselucha-Birczyńska A, Paluszkiwicz C, Chaniecki P, Błażewicz M. 2D correlation Raman spectroscopy analysis of a human cataractous lens. *Journal of Molecular Structure*. 2016;**1124**:71-77

- [16] Sacharz J, Weselucha-Birczynska A, Zięba-Palus J, Lewandowski MH, Kowalski R, Palus K, et al. Epileptic rat brain tissue analyzed by 2D correlation Raman spectroscopy. *Spectrochimica Acta Part A: Molecular and Biomolecular Spectroscopy*. 2018;**188**:581-588
- [17] Diem M, Romeo M, Boydston-White S, Miljkovic M, Matthaus C. A decade of vibrational micro-spectroscopy of human cells and tissue (1994-2004). *Analyst*. 2004;**129**:880-885
- [18] Lasch P, Boese M, Pacifico A, Diem M. FT-IR spectroscopic investigations of single cells on the subcellular level. *Vibrational Spectroscopy*. 2002;**28**:147-157
- [19] Owen CA, Notingher I, Hill R, Stevens M, Hench LL. Progress in Raman spectroscopy in the fields of tissue engineering, diagnostics and toxicological testing. *Journal of Materials Science: Materials in Medicine*. 2006;**17**:1019
- [20] Hobro AJ, Kumagai Y, Akirac S, Smith NI. Raman spectroscopy as a tool for label-free lymphocyte cell line discrimination. *Analyst*. 2016;**141**:3756-3764
- [21] Ptak W, Ptak M, Szczepanik M. *Basics of Immunology*. Warszawa: PZWL; 2017 (in Polish)
- [22] Mackiewicz S, Wiktorowicz K. *Immunology at a Glance*. Warszawa: PZWL; 1983 (in Polish)
- [23] Uzunbajakava N, Lenferink A, Kraan Y, Willekens B, Vrensen G, Greve J, et al. Nonresonant Raman imaging of protein distribution in single human cells. *Biopolymers*. 2003;**72**(1):1-9
- [24] Nakamoto K. *Infrared and Raman spectra of Inorganic and Coordination Compounds, Part B: Applications in Coordination, Organometallic, and Bioinorganic Chemistry*. 6th ed. New York: John Wiley & Sons, Inc.; 2009
- [25] Weselucha-Birczyńska A, Kozicki M, Czepiel J, Birczyńska M. Raman micro-spectroscopy tracing human lymphocyte activation. *Analyst*. 2013;**138**(23):7157-7163
- [26] Playfair JHL, Chain BM. *Immunology at a Glance*. Oxford: Blackwell Science; 2001
- [27] Dolin R. Influenza. In: Kasper DL, Fauci AS, editors. *Harrison Infectious diseases*. Vol. II. Lublin: Czelej; 2012 (in Polish)
- [28] Cohen JL. Infection with the Epstein-Barr virus. Infectious mononucleosis. In: Kasper DL, Fauci AS, editors. *Harrison Infectious Diseases*. Vol. II. Lublin: Czelej; 2012 (in Polish)
- [29] Evans DE, Munks MW, Purkerson JM, Parker DC. Resting B lymphocytes as APC for naive T lymphocytes: Dependence on CD40 ligand/CD40. *Journal of Immunology*. 2000;**164**:688-697
- [30] LeBien TW, Tedder TF. B lymphocytes: How they develop and function. *Blood*. 2008;**112**(5)
- [31] Male D, Brostoff J, Roth DB, Roitt I. *Immunology*. 2nd and 7th ed. Wrocław: Elsevier Urban & Partner; 2008

- [32] Van Wart HE, Lewis A, Scheraga HA, Saevat FD. Disulfide bond dihedral angles from Raman spectroscopy. *Proceedings of the National Academy of Sciences of the United States of America*. 1973;**70**:2619-2623
- [33] Tu AT. *Raman Spectroscopy in Biology: Principles and Applications*. New York: John Wiley & Sons; 1982
- [34] Kitagawa T, Azuma T, Hamaguchi K. The Raman spectra of Bence-Jones proteins. Disulfide stretching frequencies and dependence of Raman intensity of tryptophan residues on their environments. *Biopolymers*. 1979;**18**:451-465
- [35] Johnsen K, O'Neill JW, Kim DE, Baker D, Zhang KYJ. Crystallization and preliminary X-ray diffraction studies of mutants of B1 IgG-binding domain of protein L from *Peptostreptococcus magnus*. *Acta Crystallographica*. 2000;**D56**:506-508
- [36] Harris LJ, Skaletsky E, McPherson A. Crystallographic structure of an intact IgG1 monoclonal antibody. *Journal of Molecular Biology*. 1998;**275**:861-872
- [37] Derrick JP, Wigley DB. The third IgG-binding domain from streptococcal protein G. An analysis by X-ray crystallography of the structure alone and in a complex with Fab. *Journal of Molecular Biology*. 1994;**243**:906-918
- [38] Qian W, Krimm S. Vibrational studies of the disulfide group in proteins. *Journal of Raman Spectroscopy*. 1992;**23**:517-521
- [39] DeFranco AL. Transmembrane signaling by antigen receptors of B and T lymphocytes. *Current Opinion in Cell Biology*. 1995;**7**:163-175
- [40] Weselucha-Birczyńska A, Czepiel J, Pietruszewska M, Hola E, Moskal P, Biesiada G, et al. Human lymphocytes in infectious mononucleosis studied by Raman microspectroscopy. In: 25th International Conference on Raman Spectroscopy (ICORS 2016); 14.08.2016-19.08.2016; Fortaleza, Brazil
- [41] De Gelder J, De Gussem K, Vandenabeele P, Moens L. Reference database of Raman spectra of biological molecules. *Journal of Raman Spectroscopy*. 2007;**38**:1133-1147